

VEHICLE EXHAUST TREATMENT USING ELECTRICAL DISCHARGE AND MATERIALS CHEMISTRY

R.G. Tonkyn, M.L. Balmer, S.E. Barlow, and T.M. Orlando
Pacific Northwest National Laboratory

D. Goulette, Delphi Energy and Engine Management Systems

J.Hoard, Ford Research Laboratory

INTRODUCTION

Current "3-way" catalytic converters have proven quite effective at removing NO_x from the exhaust of spark ignition vehicles operating near stoichiometric air-to-fuel ratios. However, diesel engines typically operate at very high air-to-fuel ratios. Under such lean burn conditions current catalytic converters are ineffective for NO_x removal. As a result, considerable effort has been made to develop a viable "lean" NO_x catalyst. Although some materials have been shown to reduce NO_x under lean burn conditions, none exhibit the necessary activity and stability at the high temperatures and humidities found in typical engine exhaust. As a result, alternative technologies are being explored in an effort to solve the so-called "lean NO_x problem".

Theoretical [1,2] and experimental work [1-11] has shown that non-thermal discharges can effectively lower concentrations of both hydrocarbons and NO in gas streams, though successful treatment over the wide range of gas compositions and temperatures present in typical engine exhaust streams has yet to be demonstrated. Modeling and current experimental efforts suggest that homogeneous, gas phase remediation by discharge technology will not have the necessary energy efficiency to be practical. However, techniques that combine discharges with surface chemistry may have this potential—a fact that has recently attracted attention in the United States, Europe and Japan. Packed-bed barrier discharge systems are well suited to take advantage of plasma-surface interactions due to the large number of contaminant surface collisions in the bed. The close proximity of the active surface to transient species produced by the plasma may lead to favorable chemistry at considerably lower temperatures than required by thermal

catalysts.

We present data in this paper illustrating that the identity and surface properties of the packing material can alter the discharge-driven chemistry in synthetic leanburn exhaust mixtures. Results using non-porous glass beads as the packing material suggest the limits of NO_x reduction using purely gas phase discharge chemistry. By comparison, encouraging results are reported for several alternative packing materials.

EXPERIMENTAL

A typical dielectric barrier, packedbed reactor consists of three elements that can be assembled in a variety of ways. Two electrodes are required to create the high electric fields necessary to form a discharge at atmospheric pressure. One or both of the electrodes must be electrically isolated by a dielectric barrier to prevent direct arcing between the electrodes. In a packed-bed reactor, the volume between the electrodes is filled with a non-conductive, dielectric packing material. The packing material serves two purposes. By virtue of its shape and dielectric constant a packed bed creates numerous regions of highly amplified electric field. These regions will go into discharge at a relatively low applied voltage, and the large number of such regions helps spread the discharge throughout the entire volume of the reactor. Also, the tortuous path required for gases to traverse the bed ensures multiple contaminant-surface collisions, enhancing the possibility of favorable surface chemistry.

We utilized a cylindrical geometry reactor, consisting of a 25 mm Vycor tube, a 3.2 mm diameter stainless steel central electrode, and an outer electrode made of stainless steel tape or screen affixed tightly to the exterior of the

tube. The outer electrode was 5 cm high, giving a reactor volume of roughly 20 cm³. The position and height of the outer electrode defined the active volume, as there was no corona generated elsewhere in the reactor. The packing material of interest filled only the volume inside the outer electrode. It was held in place by a porous ceramic "washer" which rested on top of a 10 cm bed of glass beads. Electrical heating tape heated the region containing the glass beads to 10°C below the desired reaction temperature. A separate heating tape surrounded the outer electrode to maintain the desired temperature in the active portion of the reactor. Two thermocouples affixed to the outside of the reactor were used with feedback to control the bed temperature. A schematic view of our reactor is given in Figure 1.

The discharge was driven by AC voltage from a high voltage transformer (30kV/30mA). Either a variable output transformer (0 to 110 volt) operating on 60 cycle room power, or a high power audio amplifier (0-70 V, 6020,000 Hz) was used to drive the transformer.

Our discharge diagnostic system consisted of extensive gas handling facilities, power, temperature and relative humidity measurement instrumentation, a differentially pumped mass spectrometer and a chemiluminescent NO_x analyzer. For safety considerations, the reactor and high voltage power supply were housed in a vented steel cabinet. For some benchmark experiments we utilize a GC-Mass spectrometer and an FTIR spectrometer for analysis.

Accurate measurements of the power consumption in the corona reactor are critical to understanding the mechanisms of NO_x/hydrocarbon removal as well as for evaluating efficiencies and economic feasibilities. The power deposited into a barrier discharge reactor can be measured with a capacitive circuit. [12] A high voltage probe is used to measure the input voltage, and a large capacitor on the low voltage side integrates the charge transferred across the reactor per cycle.

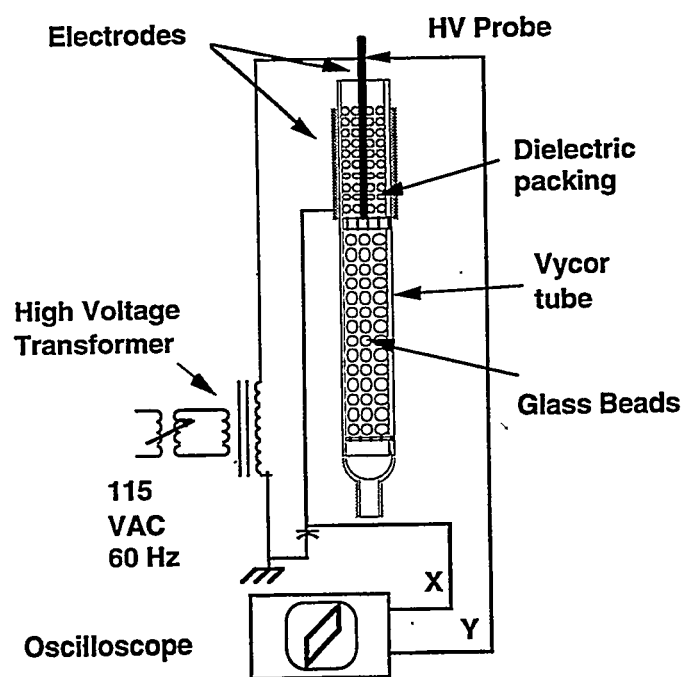


Figure 1: Schematic view of reactor and power measurement circuit. The energy per cycle is proportional to the area inside an x-y plot of the input high voltage vs. the voltage across a series capacitor.

The energy dissipated per cycle is given by:

$$E = \int_0^{\tau} P(t) dt = \int_0^{\tau} V(t) i(t) dt = \int_0^{\tau} V(t) dq(t) = C \int_0^{\tau} V(t) dV_c(t)$$

Here τ is the period of the driving wave form, P is the delivered power, V is the input high voltage, I is the current flow, q is the charge transported across the reactor, C is the capacitance of the series capacitor and V_c is the voltage across that capacitor. The integral on the right was calculated from the area inside an x-y plot of V vs. V_c over 1 period. This yielded the energy deposited in the reactor per cycle, which was converted to the average power consumption:

For most of the experiments described the simulated lean exhaust mix consisted of 7.5% oxygen, 4% CO₂, 2% H₂ O, 0.2% CO, 750 ppm C₃H₆ and 270 ppm NO. The balance was nitrogen. For some experiments nonane was used (200 ppm) instead of propane. The water content was kept at a moderate level to prevent condensation in the exhaust line or NO_x meter.

RESULTS AND DISCUSSION

Both NO and NO_x were monitored with a chemiluminescent NOX detector, with the difference attributed to NO₂ in the gas stream. In order to simplify comparisons between packing materials, the data were normalized to the inlet concentration. The data were fit assuming that the NO loss rate was first order in the energy deposited in the reactor per liter (at 298 K) of gas flow. The removal of NO_x was also assumed to be exponential, but with a non-zero final value, consistent with our observation that NO_x always appears to approach a limiting value at high energy. The equations used are as follows:

$$[NO] = [NO]_0 * e^{-E/\beta}$$

$$[NOx] = [NOx]_F + ([NOx]_0 - [NOx]_F) * e^{-E/\beta}$$

Here β is the first order decay parameter, typically in units of Joules/liter, which is commonly used to characterize and compare the energy efficiency of discharge treatment technologies. We stress that although the NO decay is first order in energy at fixed inlet conditions, the overall reaction kinetics is quite complicated. As we show below, the measured energy dependence varies with NO_x concentration. We have also observed strong dependence of β on the temperature and humidity in the gas stream.

Some plots include a line labeled "fraction reduced." What this represents is the fraction of NO loss which is not due simply to oxidation to NO₂, and is calculated by dividing the NO_x loss by the NO loss.

$$f = \frac{[NOx]_0 - [NOx]}{[NO]_0 - [NO]}$$

Since molecular nitrogen product was not detected due to the excess of N₂ in the gas stream, this fraction is an upper limit to the amount of NO which has been chemically reduced to nitrogen.

We have investigated the possible production

of other oxidative products. For example, if nitric acid were formed, we would expect a reasonable fraction to be found in water condensed from the exhaust stream. However we typically find the water to be only slightly acidic. We have found no evidence of organo-nitrate products, either with a mass spectrometer or an FTIR spectrometer. The production of N₂O is also possible, but is difficult to detect with a mass spectrometer due to the background (and product) CO₂ present. However without added CO₂ in the buffer gas, increases in the mass 44 signal appear to be correlated with the loss of propene signal (at mass 41) rather than with the NO or NO_x signal. This suggests that most of the product mass 44 arises from oxidation of propene to CO₂. In agreement with this observation, little or no N₂O was detected with the FTIR. Finally, we have looked for surface bound nitrates in post-experiment thermal analyses of our packing material. Although some nitrates are invariably observed, the amount detected is too small to explain the time-integrated quantity of NO_x which disappears.

For a limited number of experiments at a second facility we utilized an FTIR and GC-mass spectrometer to analyze the exhaust. Under typical operating conditions we saw little or no evidence of organo-nitrates, N₂O or nitric acid production. We did see a noticeable increase in CO, suggesting incomplete oxidation of the added propene. Interestingly, over a short period at least, the addition of 15 ppm SO₂ had no noticeable effect on the NO_x chemistry.

MATERIALS EFFECTS

We have investigated many different materials in our reactor, with varying results. A general observation is that there is not necessarily a good correlation between thermal activity and discharge driven activity. Figures 2a and 2b show our results for 3 separate materials in both thermal activation and in the reactor. As can be seen, the most effective material in the plasma was completely inactive for lean NO_x reduction from 100 to 500° C. This suggests that in some cases at least, the mechanism for discharge driven chemistry can be quite

different from that observed in thermal catalysis.

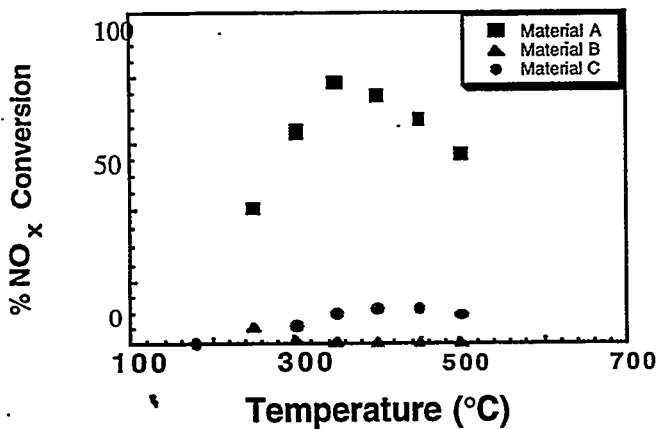


Figure 2a: Plot of the thermal activity of 3 separate materials for NO_x conversion.

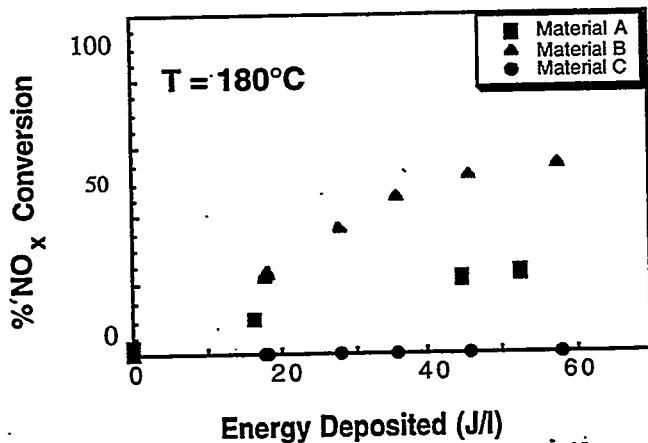


Figure 2b: Activity of the same three materials towards lean NO_x reduction in a packed bed corona reactor.

GLASS BEADS

We used non-porous glass beads as a packing material in order to study the gas phase discharge chemistry. We did not expect much, if any discharge driven surface chemistry to occur in this case, and in fact saw no evidence for it. Figures 3 and 4 illustrate our results. In Figure 3 we show a decay curve for both NO and NO_x in simulated lean exhaust as a function of the discharge energy. As can be seen, NO disappears readily, but almost all of the disappearance can be explained as oxidation of NO to NO₂. At best only 10 to 15% of the NO loss is due to chemical

reduction.

In Figure 4 we show the variation in β with the initial concentration of NO. The balance gas composition and temperature were held constant with the exception that the ratio propene to NO was held constant. The NO_x decay was limited to a few percent loss in each case. The decay of NO appears first order in energy, but the decay constant increases linearly with the concentration of NO as shown. Extrapolation of the data to low concentrations suggests a minimum value of ~ 7 J/l at extremely low concentrations. Although this result pertains only to the gas phase oxidation of NO, it illustrates the importance of characterizing energy costs under a variety of conditions. In an actual vehicle, not only the NO_x concentration but the humidity, temperature and flow velocity will be continually changing. In the long run, only tests on actual exhaust are likely to yield accurate estimates of the energy costs of discharge driven exhaust remediation.

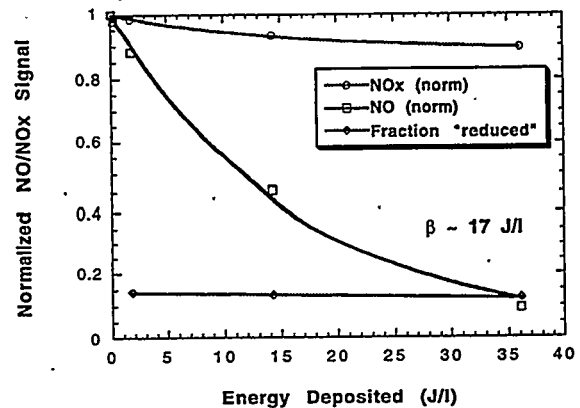


Figure 3: Plot of the normalized NO and NO_x concentrations vs energy density in Joules per liter of flow for 3 mm glass beads.

ZEOLITE MATERIALS

In general, zeolites performed well in producing clean, reproducible discharges in our reactor. For many packing materials we observe an increasing number of large voltage spikes at higher input voltages, indicative of the onset of long scale arcing between the electrode and the dielectric barrier. These spikes, which limit

the attainable energy density, are not only dangerous to the instrumentation and the reactor; they are also inefficient in creating reactive species. With zeolite packings we observed many small scale discharges, even at high input voltages, consistent with small scale surface roughness resulting in multiple high field regions near the beads.

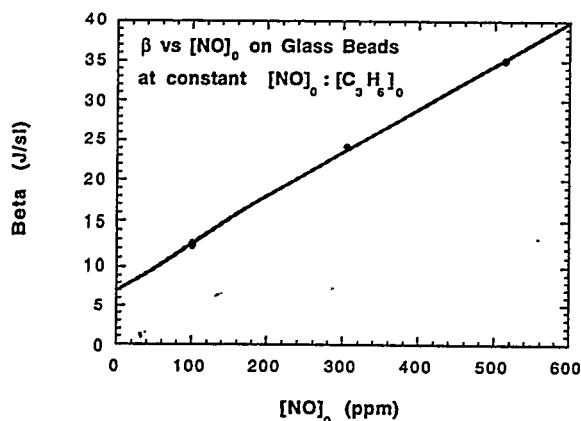


Figure 4: Variation of Beta with initial NO concentration at constant propane to NO ratio. Balance gas is simulated lean exhaust.

We report here on three different commercially available zeolites. They are labeled simply as materials A, B and C to protect their exact identity for proprietary reasons. Figure 5 illustrates data taken with material B, the most efficient material found so far. As is evident, a significant increase in the "reductive" channel was observed over that seen with glass bead packing. This is an indication that the overall chemistry has changed. Both the fraction reduced and the energy efficiency varied between the three zeolites, but their general behavior was similar. The maximum fraction of NO we have been able to "reduce" is approximately 50%, which suggests the possibility that the net reaction is a disproportionation of NO into N_2 and NO_2 . Our results for three materials are summarized in Table 1.

Examination of the energy efficiency for NO loss for many different materials indicates that the rate sometimes approaches but never exceeds that found for the (presumed) gas phase oxidation with glass beads. Furthermore, on one occasion we managed to increase the

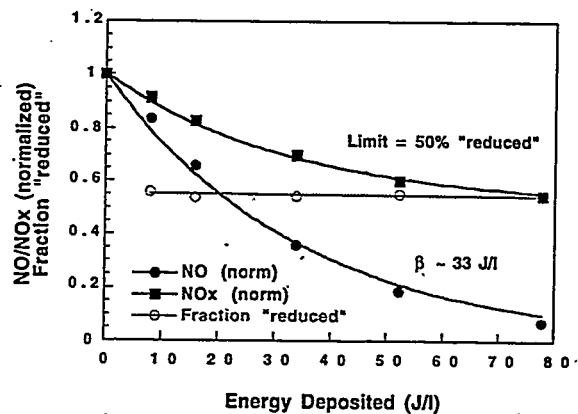


Figure 5: Plot of the normalized NO and NO_x concentrations vs. energy deposited for material B at 180°C. Approximately 45% of the NO is converted to NO_2 .

	Temp (°C)	$[NO_x]_0$ (ppm)	$\%[O_2]_0$ (ppm)	$[C_3H_8]_0$ (ppm)	β (J/l)	$[NO_x]_{t=\infty}$ (fraction)
A	160	250	5.5	780	57	0.63
B	180	270	7.3	760	34	0.5
C	180	270	7.3	760	48	0.52

Table 1: Destruction of NO in lean exhaust with Materials A, B and C.

energy beyond that required to drop the NO concentration to our detection limit. No further change was observed in the NO_x concentration at higher energies. As shown in Figure 6, oxygen enhances both the NO and NO_x decay channels, suggesting that oxidation of NO, perhaps in the gas phase, is a necessary first step in the overall discharge chemistry. A similar result is shown for the effect of added propane at constant energy in Figure 7. Interestingly, the calculated fraction of NO_x to NO loss did not vary with either added oxygen or propene. These results are similar to those observed in NO_x selective catalytic reduction studies of thermally active zeolites. [13,14] In those studies the evidence suggested that the production of N_2 from NO_x was driven by reaction of NO_2 with methane to yield both NO and N_2 product. Added oxygen enhanced the oxidation of NO to NO_2 , and added methane enhanced the subsequent reduction step.

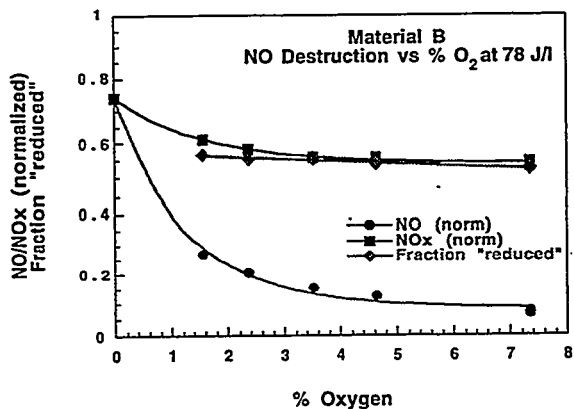


Figure 6: Plot of the normalized NO and NO_x concentrations as a function of added oxygen at constant energy on material B. The data were taken with 270 ppm NO at 180°C, with the concentrations of the other constituents held fixed

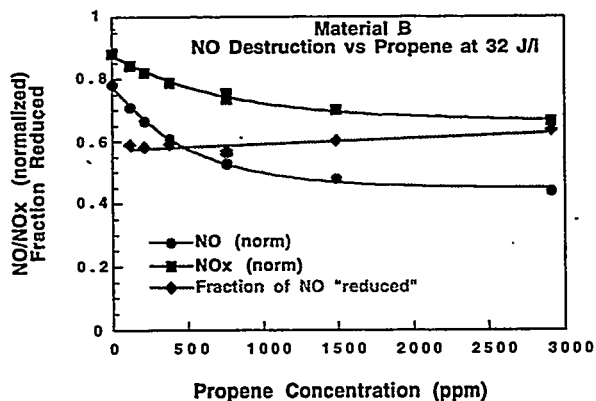


Figure 7: Plot of the normalized NO and NO_x concentrations vs. propane at constant energy on material B. The data were taken with 270 ppm NO at 215 °C, with the concentrations of the other constituents held fixed.

An obvious aspect of utilizing zeolites as a packing material is the huge available surface area. In order to investigate the effect of surface area we sintered a sample of material B for 1 hour at 800 °C. This treatment reduced the BET surface area to near zero by collapsing the pores and also changing the

phase. As can be seen in Figure 8, the observed chemistry looks quite similar to that found for glass beads. The energy efficiency for NO loss did *not* change, although the observed products did. A similar test at 700 °C only reduced the surface area by 7% without a phase change and had little effect on the chemistry.

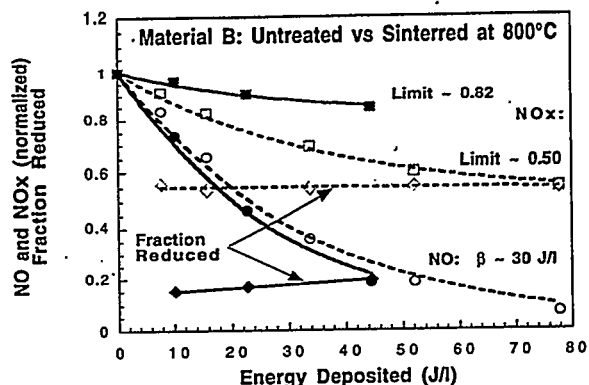


Figure 8: Comparison of material B performance before and after sintering at 800°C. The dashed lines represent the untreated material; solid lines the treated material. The loss of NO is identical, but the NO_x behavior changes considerably.

The hydrocarbons found in normal diesel exhaust tend to include higher molecular weight species than for automobile exhaust. We ran tests to determine whether a higher weight hydrocarbon would react significantly differently from propene. Figure 9 shows a comparison of the NO chemistry when we substituted ~200 ppm of nonane for 700 ppm of propene. If anything, the results for nonane are slightly better than for propane, even when considered on the basis of the carbon to NO ratio.

The increased loss of NO_x found for zeolite pack-ings could be due to plasma-assisted deposition of nitrates, nitrites or organo nitrites onto the zeolites. This has been reported to occur on γ alumina beads[15]. Certainly deposition occurs to some extent, as an excess of NO₂ is commonly observed after turning off the discharge, or upon additional heating of the

packing material. However the observed excess does not appear to be enough to explain the time-integrated loss in NO_x signal. In one experiment on material B. the time integrated loss of NO_x was measured for 13 hours of reactor operation. The beads were then removed and analysed for adsorbed nitrates by temperature programmed desorption ($100\text{-}600^\circ\text{C}$). The observed $\text{NO} + \text{NO}_2$ could only explain roughly 15% of the NO_x loss. Finally, we have never seen evidence of NO or NO_2 breakthrough.

Not all zeolites tested worked as well in the plasma reactor as the ones illustrated here. Some zeolites were not at all effective at reducing NO_x , and in fact tended to promote coke formation in the reactor, suggesting that the discharge led to surface bound graphite.

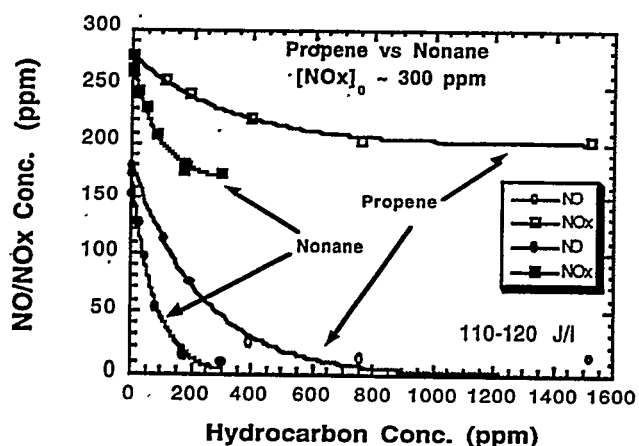


Figure 9: Comparison of the effect of added propane vs added nonane on the activity of material D for lean NO_x reduction. at fixed energy

CONCLUSION

Our data indicate that the identity of the packing material in a packed-bed dielectric barrier reactor can strongly affect the chemistry observed in the low-temperature plasma treatment of lean NO_x exhaust streams. With inactive glass beads in the reactor we show that our gas phase discharge chemistry heavily favors oxidation of NO to NO_2 over reduction. However we have found that certain zeolite materials increase what we have labeled the "reductive" channel up to 50%, a marked im-

provement from glass beads. It is plausible, but by no means proven, that this channel is indeed reduction to N_2 . We have looked for but not seen significant production of N_2O , nitric oxide or organo-nitrates in the exhaust stream. While some surface bound nitrates are seen in post-experiment analysis of the packing materials, the amount is not large enough to explain our data. The observed energy efficiency improves with increased oxygen and propene, but the branching ratio between oxidation and reduction is unchanged. Although these results are promising, progress in increasing both the energy efficiency and the fraction reduced will be necessary before a practical device can be produced.

ACKNOWLEDGMENTS

This work was supported by a Cooperative Research and Development Agreement with the Low Emissions Technology Research and Development Partnership. Pacific Northwest National Laboratory is operated for the U.S. Department of Energy by Battelle Memorial Institute under Contract No. DE-AC0676RLO 1831.

REFERENCES

- (1) Gentile, A. C.; Kushner, M. J. *J. Appl. Phys.* 1995, 78, 2074.
- (2) Penetrante, B. M.; Hsiao, M. C.; Merritt, B. T.; Vogtlin, G. E.; Wallman, P. H.; Kuthi, A.; Burkhart, C. P.; Bayless, J. R., *Appl. Phys. Lett.* 1995, 67, 3096.
- (3) Hsiao, M. C.; Merritt, B. T.; Penetrante, B. M.; Tonkyn, R. G.; Orlando, T. M., *J. Adv. Oxid. Tech.* 1996, 1, 79.
- (4) Hsiao, M. C.; Merritt, B. T.; Penetrante, B. M.; Vogtlin, G. E.; Wallman, P. H., *J. Appl. Phys.* 1995, 78, 1.
- (5) Tonkyn, R. G.; Barlow, S. E.; Orlando, T. M. *J. Appl. Phys.* 1996, 80, 4877.
- (6) Rosocha, L. A.; Anderson, G. K.; Bechtold, L. A.; Coogan, J. J.; Heck, H. G.; Kang, M.;

McCulla, W. H.; Tennant, R. A.; Wantuck, P. J. . In *Non-Thermal Plasma Techniques for Pollution Control Part B: Electron Beam and Electrical Discharge Processing*; Penetrante, B. M., Schulthies, S. E., Eds.; Springer-Verlag: Heidelberg, 1993; pp 281.

(7) Lerner, B.; Birmingham, J.; Tonkyn, R. G.; Barlow, S. E.; Orlando, T. M. *12th. Int. Symp. on Plasma Chemistry*, 1995, Minneapolis, MN.

(8) Chan, M. B.; Lee, C. C. *Environ. Sci. Technol.* 1995, 29, 181.

(9) Evans, D.; Rosocha, L. A.; Anderson, G. K.; Coogan, J. J.; Kushner, M. J. *J. Appl. Phys.* 1993, 74, 5378.

(10) Virden, J. W.; Heath, W. O.; Goheen, S.C.; Miller, M. C.; Mong, G. M.; Richardson, R. L., "*Proceedings of the Int Topical Meeting on Nuclear and Hazardous Waste Management*"; Spectrum 92, 1992, Boise, Idaho.

(11) Chang, M. B.; Kushner, M. J.; Rood, M. J., *Environ.Sci. Technol.* 1992, 777.

(12) Rosenthal, L. A.; Davis, D. A., *IEEE Trans. Ind., Appl.* 1975, I-5, 328.

(13) Lukyanov, D. B.; Lombardo, E. A.; Sill, G. A.; d'Itri, J. L.; Hall, W. K. *J. Cat.* in press.

(14) Lukyanov, D. B.; Sill, G.; d'Itri, J. L.; Hall, W. K. *J. Cat.* 1995, 153, 265.

(15) Tas, M. A.; Hardeveld, R. v.; Veldhuizen, E. M. V. van Santen, R.A, *12th International Symposium on Plasma Chemistry*, 1995, Minneapolis, MN.